energies

MDPI

Article

Multiobjective Reactive Power Optimization of Renewable Energy Power Plants Based on Time-and-Space Grouping Method

Linan Qu [1,2], Shujie Zhang [3,4], Hsiung-Cheng Lin [5,*], Ning Chen [2] and Lingling Li [1]

1 Province-Ministry Joint Key Laboratory of Electromagnetic Field and Electrical Apparatus Reliability, School of Electronic Engineering, Hebei University of Technology, Tianjin 300130, China; qulinan@epri.sgcc.com.cn (L.Q.); lilinglinglaoshi@126.com (L.L.)
2 China Electric Power Research Institute (Nanjing), Nanjing 210003, China; chen_ning@epri.sgcc.com.cn
3 School of Electrical Engineering, Xi'an University of Technology, Xi'an 710048, China; birdzsj@outlook.com
4 State Grid Qinghai Electric Power Company, Xining 810001, China
5 Department of Electronic Engineering, National Chin-Yi University of Technology, Taichung 41170, Taiwan
* Correspondence: hclin@ncut.edu.tw; Tel.: +886-42-392-4505 (ext. 7376)

Received: 25 May 2020; Accepted: 6 July 2020; Published: 10 July 2020

Abstract: The large-scale renewable energy power plants connected to a weak grid may cause bus voltage fluctuations in the renewable energy power plant and even power grid. Therefore, reactive power compensation is demanded to stabilize the bus voltage and reduce network loss. For this purpose, time-series characteristics of renewable energy power plants are firstly reflected using K-means++ clustering method. The time group behaviors of renewable energy power plants, spatial behaviors of renewable energy generation units, and a time-and-space grouping model of renewable energy power plants are thus established. Then, a mixed-integer optimization method for reactive power compensation in renewable energy power plants is developed based on the second-order cone programming (SOCP). Accordingly, power flow constraints can be simplified to achieve reactive power optimization more efficiently and quickly. Finally, the feasibility and economy for the proposed method are verified by actual renewable energy power plants.

Keywords: renewable energy generation; grid-connected; reactive power configuration; K-means++ clustering; optimal economic operation

1. Introduction

In the renewable energy power technology trend, the grid-connected renewable energy power plant is gradually built up from a low-voltage and small-scale level to a large-scale and high-voltage level. Furthermore, a cluster of renewable energy power plants, two or more neighboring renewable energy power plants that are connected to the power system via a common substation, regarded as a renewable generation cluster, is a more popular developed format in the areas with good solar resources. However, the utilization in a large-scale renewable energy generation faces a big challenge such as long-distance power transmission and large reactive loss [1–3]. Therefore, renewable energy power plants require to be configured with reactive compensation. Unfortunately, the configuration and operating cost of reactive power compensation devices still may not be sufficient so far in the industry.

According to the literature reports [4–8], most renewable energy power plants in operation use a centralized reactive power configuration scheme based on standard technical requirements in the European Union and USA. Additionally, the capacity of the reactive power equipment takes about 30% of the installed capacity of the renewable energy power plant to meet the standard requirement of voltage deviation within 5–10%. Although the current reactive power configuration methods can satisfy the limitation of voltage deviation at the grid interconnection point, it may not achieve the voltage deviation at all nodes of renewable energy power plants within a reasonable range. In other words, the configuration of reactive power as well as the economic operation of the power plants may not be working as the optimal solutions presently in power systems.

Currently, there are two main methods for studying reactive power configuration in renewable energy generation clusters. First, referring to the reactive power optimization method of the distribution network [9–12], the solution of reactive power configuration is to minimize network loss, based on the objective function of voltage stability. In the literature [13–16], based on the probabilistic idea, the scenarios of the distribution power system are cataloged to reduce the network loss with low probability in the voltage over-limit. The optimization algorithm is therefore used to solve the reactive power configuration in the distribution network [17–20]. However, the economic issue of the reactive power configuration was ignored.

Second, the reactive power configuration was configured based on the target of transient stability in the regional power grids connected with renewable energy generation [21–23]. The literature [24–26] analyzed the operation mode of the wind farm and then determined the reactive power configuration of the wind farm through the transient simulation using the typical operation mode and the limit operation mode. In this method, the reactive power configuration often ignores the cost of renewable energy generation normal operation, and greatly increases the construction and operation costs to meet system stability [27–29].

In this paper, large-scale renewable energy generation plants are taken as the research object. The typical operating curves of renewable energy generation clusters and the output characteristics of renewable energy generation units at different locations in renewable energy power plants are analyzed. Then, the chronological and spatial modeling of renewable energy power plant output is established. To minimize the renewable energy power plants' investment and operating cost, voltage stability, and the reactive power optimization configuration model in renewable energy generation clusters are solved based on the genetic algorithm.

2. Spatial Modeling of Renewable Energy Generation Cluster Based on K-Means++ Clustering Algorithm

Renewable energy generation, wind power, or photovoltaic power output can be used to estimate the power plants operating curves using the probability and statistical significance according to a large number of measured data [30,31].

The time-series data (operating data) of the renewable energy power plant is collected, with sampling interval (tm), and number (m) of samples per day. The output sample of renewable energy power plants on Day i is $\mathrm{X_i} = [\mathrm{x_{i1}}, \mathrm{x_{i2}}, \ldots\ldots, \mathrm{x_{im}}]$, and the renewable energy power plant output (X) is expressed as

$$\mathrm{X} = \begin{bmatrix} \mathrm{X_1} \\ \mathrm{X_2} \\ \vdots \\ \mathrm{X_n} \end{bmatrix} = \begin{bmatrix} \mathrm{x_{11}} & \mathrm{x_{12}} & \cdots & \mathrm{x_{1m}} \\ \mathrm{x_{21}} & \mathrm{x_{22}} & \cdots & \mathrm{x_{2m}} \\ \vdots & \vdots & & \vdots \\ \mathrm{x_{n1}} & \mathrm{x_{n2}} & \cdots & \mathrm{x_{nm}} \end{bmatrix} \tag{1}$$

where n is the number of days (samples).

Based on the K-means++ algorithm, the typical scenarios of renewable energy power plant output in one year are extracted, and the process is shown in Figure 1 and listed as follows.

Step 1: Choose a uniformly random center $\mathrm{X_i}$ of all renewable energy power plant day generation curves, and $\mathrm{X_i} = (\mathrm{x_{i1}}, \mathrm{x_{i2}}, \ldots\ldots, \mathrm{x_{im}})$ is the output sample of the renewable energy power plant on Day i;

Step 2: Calculate Euclidean distance (D_{ij}) between the sample (X_i) and the central sample (X_j);

$$D_{ij} = D(X_i, X_j) = \sqrt{\sum_{w=1}^{m} \left(x_{iw} - x_{jw}\right)^2} \quad (2)$$

where $X_j = (x_{j1}, x_{j2}, \ldots, x_{jm})$ is the output sample of the power plant on Day j. Then, calculate the sum (Sum(D)) of Euclidean distances between all samples with the center.

$$\mathrm{Sum}(D) = \sum_{j=1}^{j=n, j\neq i} D(X_i, X_j) \quad (3)$$

where Sum(D) is the sum of all Euclidean distances between samples X_j ($j = 1{:}n$, $j \neq i$) with X_i.

Step 3: Choose a new random value Rin at the range of 0 to Sum(D), and calculate $R = D(X_j)$ one by one until $R \leq 0$, and X_j is the sample except for X_i in Step 1, which is the next central sample;

Step 4: Repeat Steps 2–3 until all central samples are selected;

Step 5: Based on the selected central samples, the time groups of renewable energy power plants day–output curves are calculated through the K-means clustering algorithm, including the center for each group, which is a typical scenario of renewable energy power plants.

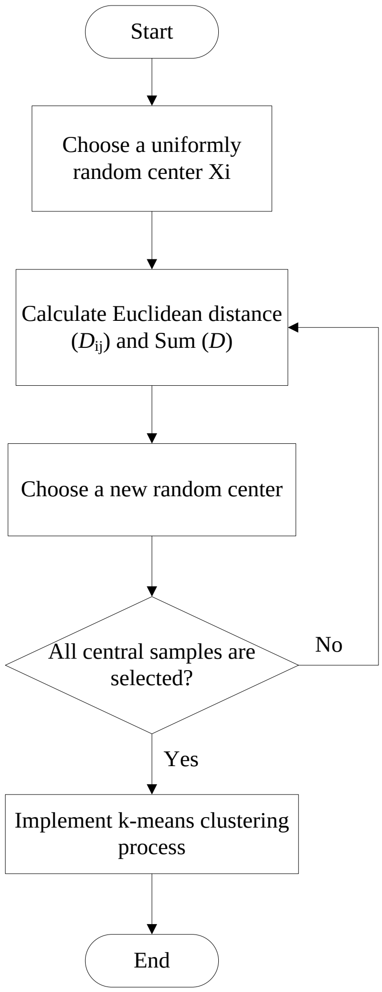

Figure 1. Flowchart of extracting typical scenarios for renewable energy power plants.

Unlike the K-means method needing to define K for the selected center sample, K-means++ method can avoid the defects of initial center deviation and fixed group size without the requirement of the K definition. The selection process ends when all central samples are selected.

Based on the number of clusters in a typical scenario, the probability of a typical scenario is defined as

$$P_{\mathrm{k}} = \frac{n_{\mathrm{k}}}{n} \tag{4}$$

where P_{k} is the probability of the typical scenario X_{k}, n_{k} is the number of samples in the X_{k} group, and n is the number of all samples.

After the time group modeling of renewable energy power plants, the K-means++ algorithm is used for the spatial clustering of renewable energy power units from one power plant or nearby power plants according to the generation output states and positions [32]. In order to optimize the configuration of reactive power compensation, it is necessary to keep the special group model consistent in each time group scenario. In other words, if the renewable power generation units are inconsistent in two typical time group scenarios, the special group would be subdivided again according to the process of extracting typical scenarios, shown in Figure 1, until it meets the requirements for each time group scenario, which is shown in Figure 2.

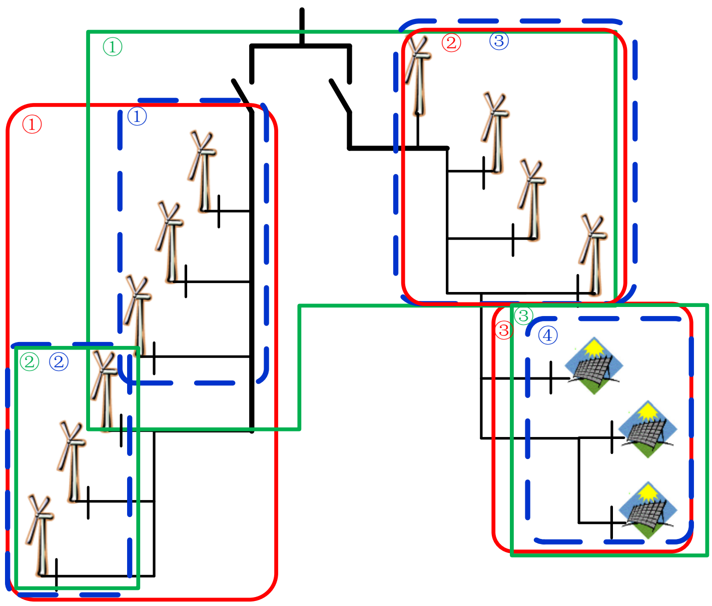

Figure 2. Spatial group modeling of renewable energy generation units.

As shown in Figure 2, the renewable power generation units are classified into three groups using a red circle according to the branches and types, while there are three subgroups using green circles according to the operating curves of renewable power generation units. Accordingly, the renewable power generation units have four subgroups in total, shown in blue circles. For each spatial cluster, we defined a node connected with the whole system.

3. Reactive Power Optimization Model

3.1. Objective Function

According to the extracting typical scenarios process, shown in Figure 1, the total power network loss of renewable energy power plants in the *k*th scenario can be obtained as

$$Loss = \sum\nolimits_{\mathrm{t}} t_{\mathrm{m}} \cdot \sum\nolimits_{\mathrm{i}} r_{\mathrm{ij}} \cdot I_{\mathrm{ij}}^{2} \tag{5}$$

where t_{m} is the sampling interval. r_{ij} is the resistance of the branch between node i and node j, and I_{ij} is the current of the branch between node i and node j. The inner sum calculates the network loss of all branches at the time t_{m}. The outer sum presents the total network loss of all time periods.

Another economic factor for the power plant operation is the cost of reactive power compensation. Set C_{unit} as the minimum capacity unit of reactive power compensation. N_{Ci} is the decision variable of the reactive power optimization configuration model for the power plant:

$$C_{\mathrm{i}} = N_{\mathrm{Ci}} \cdot C_{\mathrm{unit}} \tag{6}$$

$$C = \sum_{i} C_{\mathrm{i}} \tag{7}$$

where C_{i} is the reactive power compensation capacity at node i, and C is the sum of reactive power compensation capacity.

Then, taking the optimal economic operation of renewable energy power plants [33], the objective function of reactive power optimization is established based on the chronological scenario:

$$\text{Minimize } G = \sum_{\mathrm{k}=1}^{l} P_{\mathrm{k}}(Loss_{\mathrm{k}} + C \cdot M) \tag{8}$$

where G is the objective function; P_{k} is the probability of the kth typical scenario with a total of l scenarios; M is the investment and maintenance cost of unit capacity for reactive power. $Loss_{\mathrm{k}}$ is the total power network loss of the renewable energy power plants in the k-th scenario.

3.2. Constraints

Each typical scenario is required to meet the following constraints in renewable energy power plants. First, power balance at each time and each node should be ensured, that is to say, the active and reactive power inputs and outputs of each node are equal. Second, the active power output of each spatial clustering of renewable energy power units should not exceed its maximum value. Third, the reactive power output of each node cannot exceed the maximum capacity of its configured capacity. Fourth, the voltage of each node should be controlled within a certain range.

(1) Power flow constraints

Each spatial group of renewable power generation units is regarded as a node in the renewable energy power plants, and the power flow constraints between node i and node j are expressed as

$$\begin{cases} \sum\limits_{j \in f(i)} \left[P_{\mathrm{ij}} - r_{\mathrm{ij}} \frac{P_{\mathrm{ij}}^2 + Q_{\mathrm{ij}}^2}{V_{\mathrm{i}}^2} \right] = P_{\mathrm{iG}} - P_{\mathrm{iL}} \\ \sum\limits_{j \in f(i)} \left[Q_{\mathrm{ij}} - x_{\mathrm{ij}} \frac{P_{\mathrm{ij}}^2 + Q_{\mathrm{ij}}^2}{V_{\mathrm{i}}^2} \right] = Q_{\mathrm{iG}} + Q_{\mathrm{iC}} - Q_{\mathrm{iL}} \end{cases} \tag{9}$$

$$V_{\mathrm{i}}^2 = V_{\mathrm{j}}^2 - 2(r_{\mathrm{ij}} P_{\mathrm{ij}} + x_{\mathrm{ij}} Q_{\mathrm{ij}}) + \left(r_{\mathrm{ij}}^2 + x_{\mathrm{ij}}^2 \right) \frac{P_{\mathrm{ij}}^2 + Q_{\mathrm{ij}}^2}{V_{\mathrm{i}}^2} \tag{10}$$

where f(i) is the set of nodes in renewable energy power plants. r_{ij} and x_{ij} are the resistance and reactance of the branch between node i and node j, respectively. P_{ij} and Q_{ij} are the active and reactive power of branches between node i and node j, respectively. V_{i} and V_{j} are the voltage of node i and node j, respectively. P_{iG} and Q_{iG} are the active power and reactive power output of the renewable power generation unit group of node i. P_{iL} and Q_{iL} are the active power and reactive power of load of node i, respectively, where there is no load in the renewable energy power plants. Q_{iC} is the reactive power compensation of node i.

(2) The group output constraints of renewable power generation units

For each spatial group, the output constraints are:

$$\begin{cases} P_{\text{imin}} < P_{\text{i}} < P_{\text{imax}} \\ Q_{\text{imin}} < Q_{\text{i}} < Q_{\text{imax}} \\ \sqrt{P_{\text{i}}^2 + Q_{\text{i}}^2} < S_{\text{i}} \end{cases} \tag{11}$$

where P_{imin} and P_{imax} are the minimum and maximum active power of the spatial group of node i, respectively. Q_{imin} and Q_{imax} are the minimum and maximum reactive power of the renewable power generation unit group of node i, respectively. S_{i} is the apparent power of the spatial group of node i.

(3) Reactive power capacity constraints

For each node i, the reactive power capacity constraint defined as Q_{iC} is limited by its compensation capacity:

$$-C_{\text{i}} < Q_{\text{iC}} < C_{\text{i}} \tag{12}$$

where C_{i}, i.e., the reactive power compensation capacity, is the product of the minimum capacity unit of reactive power compensation and the decision variable of the reactive power optimization configuration model, as shown in Equation (6). It is regarded as one of the major parameters to determine the objective function in Equation (8).

(4) Voltage constraints

The voltage (V_{i}) of each node as a key parameter in the reactive power configuration should be maintained within a stable range [34,35]:

$$V_{\text{imin}} < V_{\text{i}} < V_{\text{imax}} \tag{13}$$

where V_{imax} and V_{imin} are the voltage up-limit and down-limit of node i, respectively.

3.3. Mixed-Integer Optimization Algorithm Based on Second-Order Conic Relaxation

The previous section presented the original mathematical model of the reactive power optimization configuration, which includes the nonlinear constraints Equations (9)–(11). Besides, the problem of node voltage overrun is dealt with in Equation (13).

Therefore, the proposed reactive power optimization process is achieved by the two following steps. First, the second-order conic relaxation algorithm is used to transform the load flow constraints of renewable energy power plants into second-order cone-convex constraints [36–38]. Second, the genetic algorithm is used to solve the mixed-integer model, and the optimal solution of the reactive power optimization is thus obtained.

The standard form of second-order cone programming is:

$$\text{Minimize } G_1 = \left\{ \sum_{l=1}^{\varsigma} c_l^T x_l \middle| \sum_{l=1}^{\varsigma} D_l x_l = d, x_l \in K_l, l = 1, \ldots, \varsigma \right\} \tag{14}$$

where G_1 is the object function of second-order cone programming, variable $x_l \in R_{nl}$; constant $d \in R_{n0}$, $c_1 \in R_{nl}$, $D_1 \in R_{n0\times nl}$; K_l is a second-order cone or a rotating second-order cone. Specific to this paper, R_{nl}, R_{n0}, $R_{n0\times nl}$ are the time and special groups of renewable energy generation units.

The second-order cone is expressed as:

$$K_l = \left\{ x_l \in R_{nl} \middle| x_{i,1}^2 \geq \sum_{j=2}^{n_l} x_{i,j}^2, x_{l,1} \geq 0 \right\} \tag{15}$$

A rotating second-order cone is expressed as:

$$K_l = \left\{ x_l \in R_{nl} \middle| 2x_{i,1}x_{i,2} \geq \sum_{j=3}^{n_l} x_{i,j}^2, x_{l,1}, x_{i,2} \geq 0 \right\} \tag{16}$$

The second-order cone programming is a convex one that can convert nonlinear constraints into polynomial constraints [39–41], and the error of second-order conic relaxation can be ignored [42,43]. Using the second-order cone relaxation, the nonlinear constraint of system power flow is simplified to Equation (17) to achieve the solution of the system convex set. Based on this principle, the load flow constraints of renewable energy power plants can be obtained as follows:

$$\begin{cases} \sum\limits_{j \in f(i)} \left(P_{\mathrm{ij}} - r_{\mathrm{ij}} I_{\mathrm{ij}} \right) = \sum\limits_{j \in f(i)} P_{\mathrm{ij}} + P_{\mathrm{i}} \\ \sum\limits_{j \in f(i)} \left(Q_{\mathrm{ij}} - x_{\mathrm{ij}} I_{\mathrm{ij}} \right) = \sum\limits_{j \in f(i)} Q_{\mathrm{ij}} + Q_{\mathrm{i}} \\ V_{\mathrm{i}} = V_{\mathrm{j}} - 2\left(r_{\mathrm{ij}} P_{\mathrm{ij}} + x_{\mathrm{ij}} Q_{\mathrm{ij}} \right) + \left(r_{\mathrm{ij}}^2 + x_{\mathrm{ij}}^2 \right) I_{\mathrm{ij}}^2 \end{cases} \tag{17}$$

$$I_{\mathrm{ij}} V_{\mathrm{i}} \geq P_{\mathrm{ij}}^2 + Q_{\mathrm{ij}}^2 \tag{18}$$

When solving the second-order cone relaxation problem, the constraint of Equation (18) is relaxed to be greater than or equal to the determined constraints. The error may exist during the relaxation process, but the accuracy can reach satisfactorily high.

After the second-order conic relaxation, the reactive power optimization G, defined as Equation (8), can be expressed as

$$\begin{cases} \text{Minimize } G = \sum\limits_{\mathrm{k}=1}^{l} P_{\mathrm{k}} (Loss_{\mathrm{k}} + C \cdot M) \\ \text{ct : Equations} \quad (16), (17) \\ \text{Equations} \quad (6), (7), (12) \\ \text{Equations} \quad (11), (13) \end{cases} \tag{19}$$

where Equation (19) implies that Equation (8) is the objective function for reactive power optimization with constraint functions Equations (16), (17), (6), (7), (11), (12) and (13).

In the second step, the genetic algorithm is used to reach the optimization solution, and the process is shown in Figure 3.

Step 1: Initialization: Problem complexity and problem size can be taken into account when the number of initial samples is decided.

Step 2: Fitness calculation: The fitness function is used to evaluate the goodness of the chromosomes (samples). It is defined using the objective function to optimize the economy of renewable energy power plants, as shown in Equation (8).

Step 3: Reproduction and crossover: Select the chromosomes into the mating pool, and crossover operation is used to perform on chromosomes, including single-point crossover, two-point crossover, uniform crossover, order crossover, and some others.

Step 4: Mutation: The operation is used to perform on chromosomes, including bitwise mutation, insert mutation, inversion mutation, scramble mutation, swap mutation, and some others. Appropriate mutation operators can be selected by taking problem and chromosome representation into account.

Step 5: Stopping criteria: If the predefined number defined in Step 1 is reached, the calculation process will stop. Take the greatest fitness obtained in the evolution process as the optimal solution.

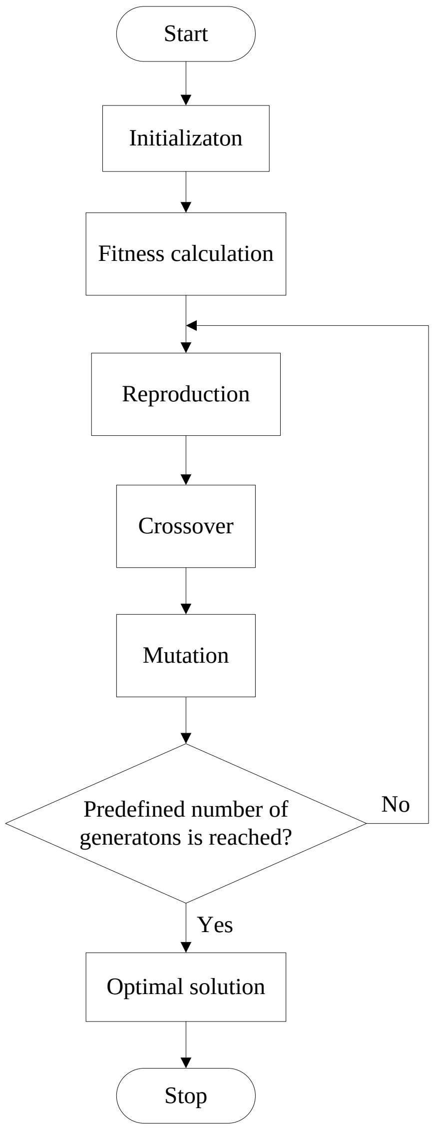

Figure 3. Process of genetic algorithm.

4. Performance Results

There were two wind farms and one photovoltaic power plant used to carry out calculation analysis in this study. The scenario from large-scale renewable energy power plants remotely connected to the power grid in Xinjiang, China, was used to verify the effectiveness of the proposed model. The installed capacity of wind farms and photovoltaic power plants is 50 MW, 100 MW, and 150 MW, and the diagram of which is shown in Figure 4.

Using K-means++ clustering algorithm, the renewable energy power plants' operation curves are group modeling into six typical scenarios, and each scenario has a central sample. Figure 5 is a typical scenario of a renewable energy generation plant containing wind farms and photovoltaic power plants. It shows the center sample of typical scenarios after time group modeling. On the other hand, the probability of typical scenarios is shown in Figure 6, which is used for calculating the annual loss in Table 1.

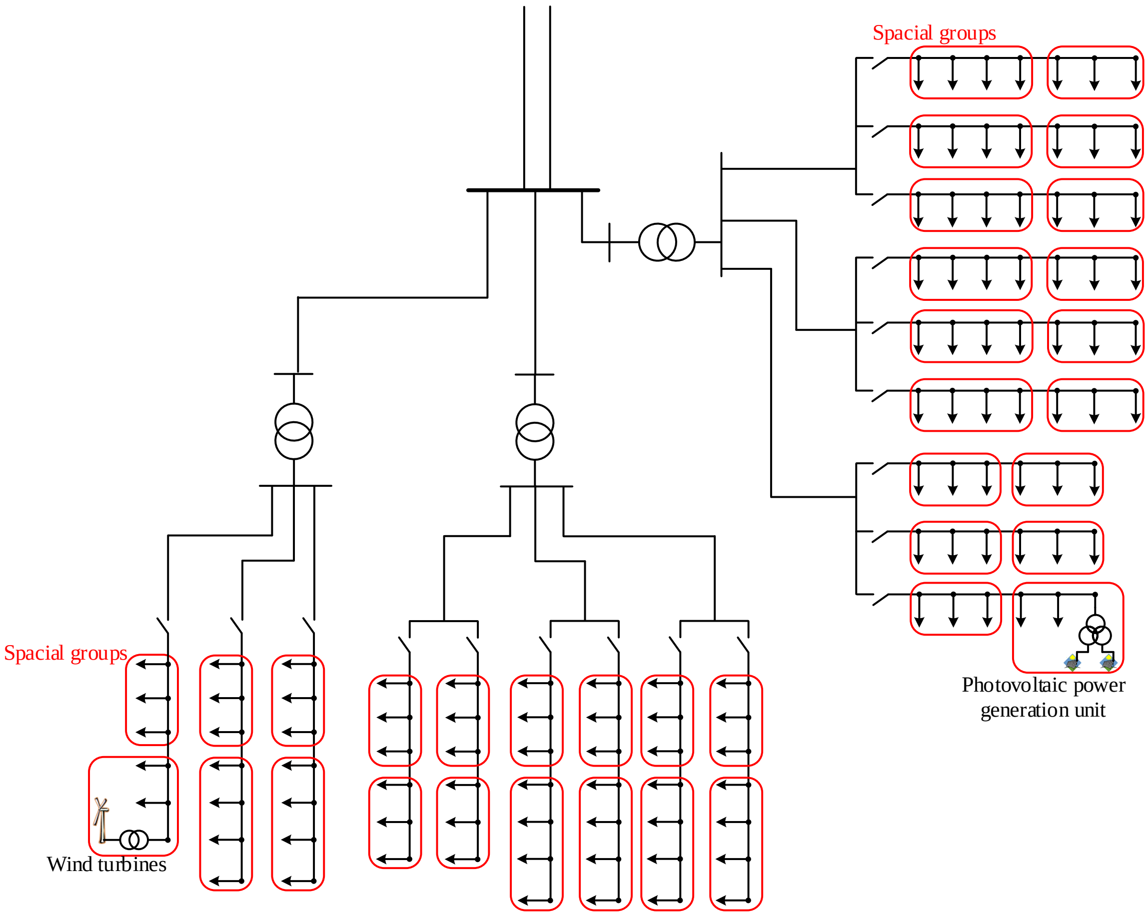

Figure 4. Diagram of renewable energy power plants of the case.

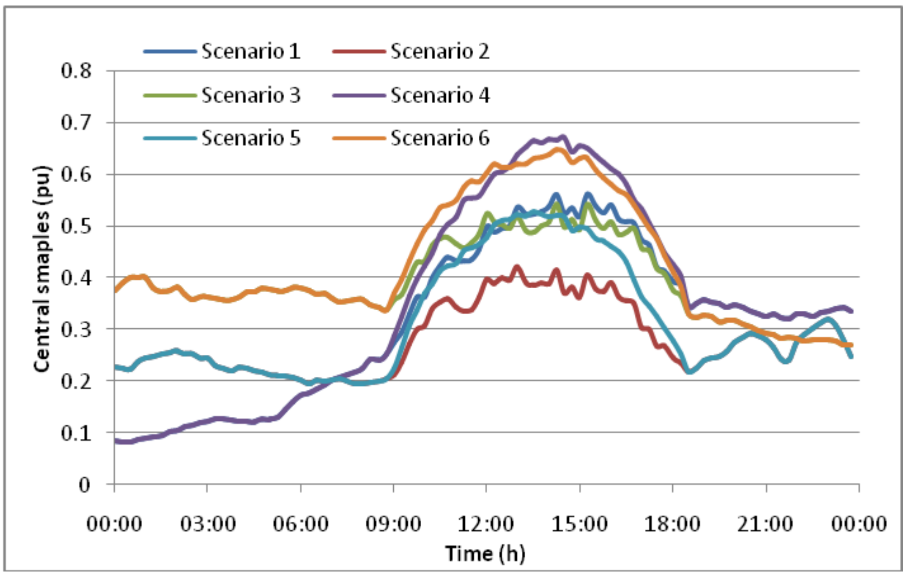

Figure 5. Time group samples of renewable energy power plants.

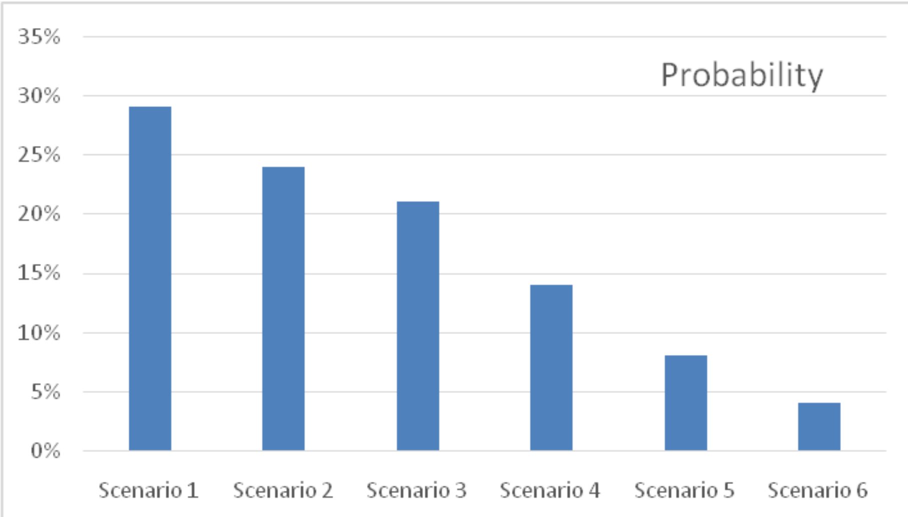

Figure 6. Probability of time group scenarios of renewable energy power plants.

According to the time group model and electrical location, renewable power generation units are grouped on scenarios, and the final spatial group model of renewable power generation units is shown in red circles of Figure 4. The renewable energy power plants include two wind farms and one photovoltaic power plant, contain three feeders, six feeders, and nine feeders, respectively; and each feeder contains 6–7 renewable power generation units. After the time-and-space group model, each feeder is divided into two renewable power generation unit groups. Therefore, the simplified diagram of renewable energy power plants for reactive power optimization is defined in Figure 7.

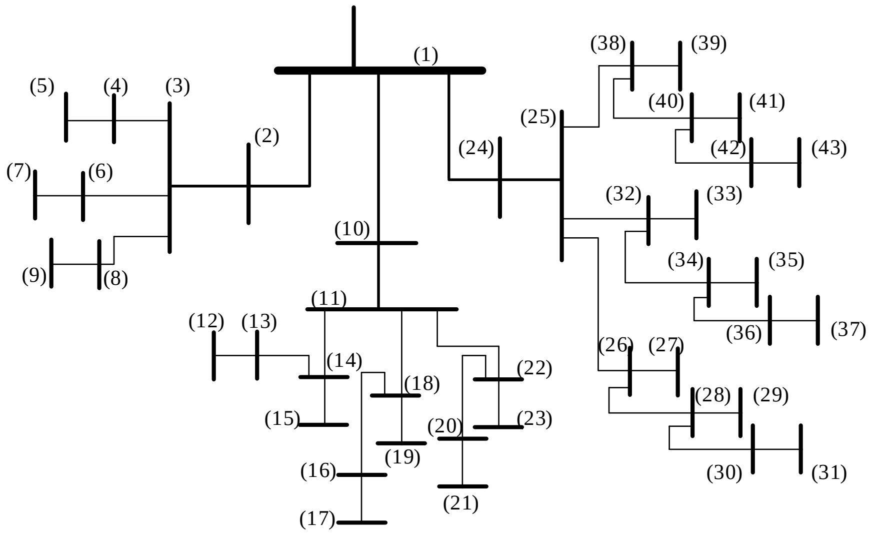

Figure 7. Simplified diagram of renewable energy power plants for reactive power optimization.

As mentioned in the opening paper, there are two main methods for studying reactive power compensation in renewable energy generation plants, minimize operation network loss [18,20] and transient stability. The cost of reactive power compensation is not included in the targets of the mentioned methods. The result of network loss and static var generator (SVG) cost is shown in Table 1.

Table 1. Reactive capacity configuration according to minimize operation network loss target.

Location	Capacity (MW)	The Whole Year Network Loss (MWh)	SVG Cost and Loss Cost, Solution from Equation (19)	Maximum Voltage Deviation (p.u.)
(1)	20	19,261.7	18,375.01	1.50%
(3)	5			
(11)	12			
(22)	5			
(25)	20			
(36)	5			
(42)	2.5			

Note 1: Investment and maintenance cost of unit capacity for reactive power: US$14.17 dollar/kVar; Note 2: Renewable energy power tariff: US$0.07 dollar/kWh [44].

In the study, the reactive power compensation configuration methods can be classified into two major objectives as follows. The first method aims to reach the lowest network loss in the operation of renewable energy power plants. Therefore, in Equation (13), the voltage deviation of each type of bus node tends to maintain the smallest value. This ensures that the network loss is minimal when renewable power is sent out to the grid connection. The second method, considering the operation stability of the renewable energy power plant as the first priority, the reactive power compensation attempts to meet the voltage control as much as possible, that is, the Equation (13) is regarded as the control target. Generally, in these two methods, the obtained reactive power compensation scheme remains the same, and the voltage deviation of each node of the renewable energy power plant can be controlled within 1.5%.

The minimization of network loss and SVG cost in this study in each typical scenario and multi scenario with probability is shown in Table 2. It is obvious that the economy of multi scenario result is better than Table 1.

Table 2. Reactive capacity optimization results in each scenario.

Evaluation Item	Location	Capacity (MW)	The Whole Year Network Loss (MWh)	SVG Cost and Loss Cost, Solution from Equation (19)	Maximum Voltage Deviation (p.u.)
Scenario 1	(1)	20	17,677.37	11,536.91	2.00%
	(3)	5			
	(11)	12			
	(22)	7			
	(25)	9			
	(36)	4.5			
Scenario 2	(1)	5.5	12,491.85	8066.01	5.00%
	(3)	5.4			
	(11)	10			
	(25)	18			
Scenario 3	(1)	17	25,240.58	14,877.88	2.50%
	(3)	5.2			
	(11)	12			
	(22)	7			
	(25)	9			
Scenario 4	(1)	20	23,884.46	13,853.38	3.80%
	(3)	4			
	(11)	7			
	(25)	12			
Scenario 5	(1)	6.9	15,956.82	9843.84	3.00%
	(3)	5.6			
	(11)	10			
	(25)	18			

Table 2. *Cont.*

Evaluation Item	Location	Capacity (MW)	The Whole Year Network Loss (MWh)	SVG Cost and Loss Cost, Solution from Equation (19)	Maximum Voltage Deviation (p.u.)
Scenario 6	(1) (3) (11) (22) (25) (36) (42)	20 5 12 5 20 5 2.5	30,408.18	18,375.01	1.50%
Multiscenario with probability	(1) (3) (11) (25)	19 5 12 18	16,768.82	10,916.72	2%

As above, it can be observed that the investment of multi scenario reactive compensation is not the lowest one among six scenarios. On the other hand, owing to the voltage constraints, the maximum value of the voltage deviation of the multi scenario is less than 2% [45,46]. However, the maximum voltage deviation ranges between 1.8% and 5% due to the influence of other scenarios.

Comparing Tables 1 and 2, the configuration scheme of Table 1 is relevant to Scenario 6 in Table 2. In this research, multi scenario with probability targeted at all scenarios, the voltage control accuracy is slightly sacrificed, that is, the voltage deviation increases from 1.5% to 2% to maximize the economic benefit. Nevertheless, the voltage control accuracy is still satisfactory in the grid operation requirements, i.e., ±5% [4–8] under overall optimization consideration in the construction cost of the reactive power compensation.

5. Conclusions

After analyzing the demand for reactive power for large-scale renewable energy power plants, the time-and-space grouping model has been established successfully. The proposed method is to reduce investment and loss costs with the premise of the stable operation of renewable energy generation. The key contribution of this approach is different from the ones already developed and used successfully in the EU and USA. First, the typical scenarios of renewable energy power plant output and the probability, as time modeling, are extracted using the K-means++ algorithm. The spatial clustering of renewable energy power units is then built in one power plant or nearby power plants, according to typical scenarios and electrical positions of the renewable power generation unit. The time-and-space grouping model of renewable energy power plants is therefore constituted.

Second, taking the optimal economic operation of renewable energy power plants, the objective function of reactive power optimization is established based on the time-and-space grouping model, including four major constraints, i.e., power balance, output limitation of renewable power generation, reactive power capacity limitation, and voltage operation limitation. Among them, the power flow constraint is relaxed to second-order cone-convex constraint due to the nonlinear characteristics, and reactive power optimization is solved by genetic algorithms.

Consequently, reactive power compensation optimization considering crucial constraints such as power balance, renewable power generation unit output, and voltage deviation in renewable energy power plants has been achieved. In this paper, the renewable energy power plants with the capacity of 300 MW were studied, and some key contributions are listed as follows.

(1) The proposed model has taken account of full-cycle time characteristics and used a smaller number of samples from 35,040 to 384. Additionally, the number of network nodes has been reduced from 127 to 43.

(2) The reactive power optimization model with an optimal economic operation is achieved. The complex power flow constraints are simplified into a convenient second-order cone model, which reduces the number of iterations of nonlinear optimization problems.

Additionally, it is found that the voltage of each node in the renewable energy generation plant plays a key role in the reactive power configuration. Accordingly, the future research of this paper would move forward to the control of voltage constraints under high renewable energy resources penetration in a network. Furthermore, the condition of the network with the stability of the nod may affect the reactive power controlling method, especially in very large wind systems of rather weak networks. This issue is more complex in this field, and it would be established as a subsequent research objective.

Author Contributions: L.Q., S.Z. and N.C. developed the optimization method, collected the data and performed analysis. H.-C.L. and L.L. helped edit the manuscript. All authors contributed to the writing of the paper. All authors have read and agreed to the published version of the manuscript.

Funding: This study was supported by the science and technology project of State Grid Corporation of China (Research on Key Technologies of Power Grid Coordination of HVDC send-side for All-Clean Energy Power), and the key project of Tianjin Natural Science Foundation of China [Project No. 19JCZDJC32100].

Conflicts of Interest: The authors declare no conflict of interest.

References

1. Yuan, X. Integrating Large Wind Farms Into Weak Power Grids With Long Transmission Lines. *Trans. China Electrotech. Soc.* **2007**, *22*, 29–36.
2. Piwko, R.; Miller, N.; Sanchez-Gasca, J.; Yuan, X.; Lyons, J. Integrating Large Wind Farms into Weak Power Grids with Long Transmission Lines. In Proceedings of the 2005 IEEE/PES Transmission & Distribution Conference & Exhibition: Asia and Pacific, Dalian, China, 14–16 August 2006; pp. 1–7.
3. Li, L.; Zhao, X.; Tseng, M.; Tan, R. Short-term wind power forecasting based on support vector machine with improved dragonfly algorithm. *J. Clean. Prod.* **2020**, *242*, 118447. [CrossRef]
4. Association for Electrical, Electronic and Information Technologies. *Technical Requirements for the Connection and Operation of Customer Installations to the High-Voltage Network VDE*; VDE–AR–N 4120:2015–01; Association for Electrical, Electronic and Information Technologies: Frankfurt, Germany, 2018.
5. *The Grid Code*; Issue 5 Version 45; National Grid Electricity System Operator Limited: London, UK, June 2020.
6. ENTSO-E (European Network of Transmission System Operators). *Network Code for Requirements for Grid Connection Applicable to All Generators*; ENTSO-E: Brussels, Belgium, March 2013.
7. CEPRI (China Electric Power Research Institute). *Technical Rule for Connecting Wind Farm to Power System (GB/T 19963)*; CEPRI: Beijing, China, 2011.
8. CEPRI (China Electric Power Research Institute). *Technical Requirements for Connecting Photovoltaic Power Station to Power (GB/T 19964)*; CEPRI: Beijing, China, 2012.
9. Xioa, H.; Pei, W.; Dong, Z.; Pu, T.; Chen, N.; Kong, L. Reactive Power Optimization of Distribution Network with Distributed Generation Using Metamodel-based Global Optimization Method. In Proceedings of the 2018 Annual Meeting of the Canadian Society of Ecology and Evolution (CSEE2018), Guelph, ON, Canada, 18–21 July 2018.
10. Guo, Q.; Wu, J.; Mo, C.; Xu, H. A Model for Multi-objective Coordination Optimization of Voltage and Reactive Power in Distribution Networks Based on Mixed Integer Second-order Cone Programming. In Proceedings of the 2018 Annual Meeting of the Canadian Society of Ecology and Evolution (CSEE2018), Guelph, ON, Canada, 18–21 July 2018.
11. Xie, J.; Liang, C.; Xiao, Y. Reactive Power Optimization for Distribution Network Based on Distributed Random Gradient-Free Algorithm. *Energies* **2018**, *11*, 534. [CrossRef]
12. Caramanis, M.; Ntakou, E.; Hogan, W.; Chakrabortty, A.; Schoene, J. Co-Optimization of Power and Reserves in Dynamic T&D Power Markets with Nondispatchable Renewable Generation and Distributed Energy Resources. *Proc. IEEE* **2016**, *104*, 807–836.
13. Zeng, X.; Tao, J.; Zhang, P.; Pan, H.; Wang, Y. Reactive Power Optimization of Wind Farm based on Improved Genetic Algorithm. *Energy Procedia* **2012**, *14*, 1362–1367. [CrossRef]

14. Calderaro, V.; Galdi, V.; Piccolo, A.; Conio, G.; Fusco, R. Wind Farm Power Plant: Optimal Capacitor Placement for Reactive Power Compensation. In Proceedings of the 4th IEEE PES Innovative Smart Grid Technologies Europe (ISGT Europe), Copenhagen, Denmark, 6–9 October 2013; pp. 1–5.
15. Kiamehr, K.; Hannani, S. Wind farm layout optimization using imperialist competitive algorithm. *J. Renew. Sustain. Energy* **2014**, *6*, 043109. [CrossRef]
16. Ding, T.; Liu, S.; Yuan, W.; Bie, Z.; Zeng, B. A Two-Stage Robust Reactive Power Optimization Considering Uncertain Wind Power Integration in Active Distribution Networks. *IEEE Trans. Sustain. Energy* **2016**, *7*, 301–311. [CrossRef]
17. Tu, R.; Zhao, C.; Liu, Z.; Cui, Y.; Xie, W.; Zhou, D. Research of reactive power control strategy to reduce the reactive power exchange of AC and DC power grid. *J. Eng.* **2017**, *13*, 751–755.
18. Zhang, C.; Chen, H.; Shi, K.; Liang, Z.; Mo, W.; Hua, D. A Multi-time Reactive Power Optimization Under Interval Uncertainty of Renewable Power Generation by an Interval Sequential Quadratic Programming Method. *IEEE Trans. Sustain. Energy* **2019**, *10*, 1086–1097. [CrossRef]
19. Arefifar, S.; Mohamed, Y. Probabilistic Optimal Reactive Power Planning in Distribution Systems With Renewable Resources in Grid-Connected and Islanded Modes. *IEEE Trans. Ind. Electron.* **2014**, *61*, 5830–5839. [CrossRef]
20. Zhang, C.; Chen, H.; Liang, Z.; Guo, M.; Hua, D.; Ngan, H. Reactive Power Optimization Under Interval Uncertainty by the Linear Approximation Method and Its Modified Method. *IEEE Trans. Smart Grid* **2018**, *9*, 4587–4600. [CrossRef]
21. Xu, X.; Chen, Q. Research on reactive power compensation algorithm based on game theory in wind farm. *Key Eng. Mater.* **2010**, *439–440*, 989–993. [CrossRef]
22. Keane, A. Information gap decision theory based congestion and voltage management in the presence of uncertain wind power. *IEEE Trans. Sustain. Energy* **2016**, *7*, 841–849.
23. Liu, L.; Li, H.; Xue, Y.; Liu, W. Reactive Power Compensation and Optimization Strategy for Grid-Interactive Cascaded Photovoltaic Systems. *IEEE Trans. Power Electron.* **2015**, *30*, 188–202. [CrossRef]
24. Cao, J.; Zhang, W.; Xiao, Z.; Hua, H. Reactive Power Optimization for Transient Voltage Stability in Energy Internet via Deep Reinforcement Learning Approach. *Energies* **2019**, *12*, 3390. [CrossRef]
25. Huang, Q.; Vittal, V. Application of electromagnetic transient-transient stability hybrid simulation to FIDVR study. *IEEE Trans. Power Syst.* **2016**, *31*, 2634–2646. [CrossRef]
26. Yang, H.; Liao, J. MF-APSO-Based Multiobjective Optimization for PV System Reactive Power Regulation. *IEEE Trans. Sustain. Energy* **2015**, *6*, 1346–1355. [CrossRef]
27. Rather, Z.; Chen, Z.; Thøgersen, P.; Lund, P. Dynamic Reactive Power Compensation of Large-Scale Wind Integrated Power System. *IEEE Trans. Power Syst.* **2015**, *30*, 2516–2526. [CrossRef]
28. Bonfiglio, A.; Brignone, M.; Delfino, F.; Procopio, R. Optimal Control and Operation of Grid-Connected Photovoltaic Production Units for Voltage Support in Medium-Voltage Networks. *IEEE Trans. Sustain. Energy* **2014**, *5*, 254–263. [CrossRef]
29. Jin, D.; Chiang, H.; Li, P. Two-Timescale Multi-Objective Coordinated Volt/Var Optimization for Active Distribution Networks. *IEEE Trans. Power Syst.* **2019**, *34*, 4418–4428. [CrossRef]
30. Arthur, D. K-means++: The advantages of careful seeding. In Proceedings of the Eighteenth Annual ACM-SIAM Symposium on Discrete Algorithms, New Orleans, LA, USA, 7–9 January 2007.
31. Lin, L.; Pan, X.; Zhang, L.; Zhao, S. The K-means Clustering Algorithm for Wind Farm Based on Immune-outlier Data and Immune-sensitive Initial Center, k-means clustering algorithm. In Proceedings of the World Congress on Civil, Structural, and Environmental Engineering (CSEE 2016), Prague, Czech Republic, 30–31 March 2016.
32. Liu, M.; Pan, W.; Zhang, Y.; Zhao, K.; Zhang, S.; Liu, T. A Dynamic Equivalent Model for DFIG-Based Wind Farms. *IEEE Access* **2019**, *7*, 74931–74940. [CrossRef]
33. Alkaabi, S.; Zeineldin, H.; Khadkikar, V. Short-Term Reactive Power Planning to Minimize Cost of Energy Losses Considering PV Systems. *IEEE Trans. Smart Grid* **2019**, *10*, 2923–2935. [CrossRef]
34. Hatziargyriou, N.; Karakatsanis, T.; Lorentzou, M. Voltage control settings to increase wind power based on probabilistic load flow. In Proceedings of the 2004 International Conference on Probabilistic Methods Applied to Power Systems, Ames, IA, USA, 12–16 September 2004.
35. Koutsoukis, N.; Georgilakis, P.; Hatziargyriou, N. Active distribution network planning based on a hybrid genetic algorithm-nonlinear programming method. *Open Access Proc. J.* **2017**, *1*, 2065–2068. [CrossRef]

36. Bonami, P.; Biegler, L.; Conn, A. An algorithmic framework for convex mixed integer nonlinearprograms. *Discret. Optim.* **2008**, *5*, 186–204. [CrossRef]
37. Liu, J.; Liu, S. Optimal Distributed Generation Allocation in Distribution Network Based on Second Order Conic Relaxation and Big-M Method. *Power Syst. Technol.* **2018**, *8*, 2604–2611.
38. Farivar, M.; Low, S. Branch flow model: Relaxations and convexification—Part I. *IEEE Trans. Power Syst.* **2013**, *28*, 2554–2564. [CrossRef]
39. Li, J.; Xin, H.; Wei, W.; Dai, W. Decentralized conic optimization of reactive power considering uncertainty of renewable energy sources. *IET Renew. Power Gener.* **2016**, *10*, 1348–1355. [CrossRef]
40. Hong, S.; Cheng, H.; Zeng, P.; Zhang, J.; Lu, J. Composite generation and transmission expansion planning with second order conic relaxation of AC power flow. In Proceedings of the 2016 IEEE PES Asia-Pacific Power and Energy Engineering Conference (APPEEC), Xi'an, China, 25–28 October 2016.
41. Baradar, M.; Hesamzadeh, M. AC Power Flow Representation in Conic Format. *IEEE Trans. Power Syst.* **2015**, *30*, 546–547. [CrossRef]
42. Chen, J.S. Two classes of merit functions for the second-order cone complementarity problem. *Math. Methods Oper. Res.* **2006**, *64*, 495–519. [CrossRef]
43. Pan, S.; Kum, S.; Lim, Y. On the generalized Fischer Burmeister merit function for the second-order cone complementarity problem. *Math. Comput.* **2014**, *83*, 1143–1171. [CrossRef]
44. National Development and Reform Commission. *Notice on Adjusting the On-Grid Electricity Price of Photovoltaic Power Generation Onshore Wind Power*; National Development and Reform Commission: Beijing, China, 26 December 2016.
45. Gianfreda, A.; Parisio, L.; Pelagatti, M. Revisiting long-run relations in power markets with high RES penetration. *Energy Policy* **2016**, *94*, 432–445. [CrossRef]
46. Anastasiadis, A.; Kondylis, G.; Papadimitriou, C.; Polyzakis, A.; Vokas, G.; Psomopoulos, C. Maximum Power Photovoltaic Units Penetration under Voltage Constraints Criteria in Distribution Network Using Probabilistic Load Flow. *Energy Procedia* **2019**, *157*, 578–585. [CrossRef]